Physics with an Electron-positron Storage Ring of Beam Energy E = 14 GeV

EPIC Working Party 1, May 1974

For the energy region under consideration, the electron-positron system can be used to study a wide range of fundamental physical interactions. We consider them under a series of headings.

a) Hadron production in electron-positron annihilation.

This area of phenomena is "terra incognita" at present. Its exploration will have the greatest importance for our comprehension of the deepest and most fundamental hadronic interactions.

Because of the smallness of the electromagnetic coupling, these interactions are dominated by the one-photon annihilation process depicted in Fig. 1(a). Therefore, these processes pass through an intermediate state limited to the spatial quantum numbers (JPC) = (1--). The final states reached are very restricted relative to those reached in antiproton-proton annihilation, for example. This restriction will lead to some simplicities in the phenomena. Further, we believe that the electromagnetic (EM) interaction has a special simplicity, a belief which will be tested by parallel experiments.

The "orthodox view" up to the present has been that based on the parton model. This model has had great success in the interpretation of electron-nucleon scattering and neutrino-nucleon interactions in the deep inelastic regime, as well as of proton proton interactions at the highest energies. It is now in some difficulty with the data from E = 1 GeV to E = 2.5 GeV from CEA and SPEAR. This orthodox view leads to the expectation that the ratio

$$R((2E)^2) = \left\{\sigma\,(e^+e^- \to \text{hadrons})/\sigma\,(e^+e^- \to \mu^+\mu^-)\right\} \to \sum_i (Q_i^2) \qquad (1)$$

approaches a constant in the limit of infinitely high E, where Q_i denotes the charge of the parton of type i. This sum takes the value 2/3 for the Gell-Mann-Zweig quark model, 2 for the three-colour-triplets model (fractional charges), and 4 for the Han-Nambu three-triplet model (integral charged quarks). The energy-dependence which has recently been established for R is shown on Fig. 2. R rises essentially linear in E^2, from a value of 2 at E = 1 GeV to the value 6 at E = 2.5 GeV, in contradiction to these expectations.

At this point, it is convenient to recall that, on the basis of quantum electrodynamics (QED),

$$\sigma\,(e^+e^- \rightarrow \mu^+\mu^-) = \frac{\pi\alpha^2}{3E^2} = \frac{21.7}{E^2}\ \text{nb. GeV.}^{-2} \qquad (2)$$

This expression has now been checked experimentally up to E = 2.5 GeV at SPEAR.

The energy dependence observed for the total cross section $\sigma\,(e^+e^- \rightarrow$ hadrons) is shown on Fig. 3; it is compatible with a constant value of about 22 nb. It is quite unclear how these data will extrapolate to the EPIC energies. The only thing that is clear is that this total cross section must start to fall at some high energy E'. The vacuum polarization corrections to the photon propagator $1/q^2$, arising from this hadron production, are given by the propagator form

$$D(q) = \frac{1}{q^2}\left\{1 - \frac{1}{3\pi}\, q^2 \int_{4m^2_\pi}^{\infty} \frac{d\sigma^2 R(\sigma^2)}{\sigma^2(\sigma^2 - q^2)} + \ldots\right\} \qquad (3)$$

If $R(q^2)$ continued to rise linear in q^2, the expression within the brackets of (3) would no longer be convergent, which would represent a major upset for QED; at the very least, the renormalization program for QED would no longer be possible. Even if $R(q^2)$ continued to increase linearly up to the EPIC energy E' = 14 GeV

and then became constant, these corrections would give rise to quite strong deviations from QED (amounting to $\approx 10\%$ in amplitude for $E = 9$ GeV). Experiments with EPIC will therefore establish either non-constancy for $\sigma(e^+e^- \rightarrow \text{hadrons})$ or substantial deviations from QED.

From the arguments put forward by Drell and Chanowitz concerning finite-size effects for partons, and their extensions by West to include magnetic moment effects, it appears an interesting possibility that these data may indicate that e^+e^- experiments are beginning to probe the structure of the partons. Further, this may well be bound up with the detailed properties of (vector-meson) gluons, if such exist, in which case the data in Fig. 2 may represent the beginning of an approach to a resonance state at energy E^* corresponding to some gluon mass value $M^* = 2E^*$. Even if this resonance state exists only for some mass value far beyond the energy of EPIC, the study of the behaviour of this cross section will clearly still be a vital clue to these phenomena. The first purpose of the EPIC experimental programme, and the primary justification for the construction of EPIC, is the exploration and analysis of precisely this unknown region of phenomena.

The study of the decay of the hadronic matter generated by the intermediate photon from the e^+e^- annihilation will also be of the greatest interest:

(i) All inclusive cross sections, i.e. the momentum spectra for each kind of particle emitted, for π's, K's, protons and other baryons, for ρ-mesons, for Δ particles, and so on, must be studied as function of production direction θ, as function of incident energy E. Their relationship with those observed following $\bar{p}$-p annihilation will be especially interesting. The preliminary indications at SPEAR are that the pion spectra have little dependence on θ, being given by the form

$$E \frac{d\sigma}{d^3p} \sim \exp(-6p), \qquad (4)$$

when p is measured in GeV/c. This momentum dependence happens to fit well also the $(p_\perp)_\pi$ distribution in pp collisions at the ISR and the p_π distribution in $\bar{p}p$ annihilation. It is contrary to the "orthodox views" which suggest that the e^+e^- annihilation process should be dominated by the formation of two oppositely-directed "jets" and which therefore require quite a different spectral form. Much of this data will have a rather direct connection with the structure functions for deep-inelastic (e,e') reactions on p and π, although in a different domain for the physical variables.

(ii) At the other extreme, the structure of complete final states will also have the greatest interest, in view of this parton-model expectation of a "two-jet" structure. Other structures are possible, for example a multi-fireball or multi-jet structure, or a diffuse (single fireball) structure; the SPEAR inclusive data already gives some indications for the latter possibility. More generally, the study of correlations between pairs (and larger groups) of outgoing particles will also give us important clues concerning the nature of the state of hadronic matter formed. It is worth emphasizing here that the hadronic matter resulting from e^+e^- annihilation has definite quantum numbers, JPC = 1--. This contrasts greatly with the hadronic matter formed through other processes. $\bar{p}p$ annihilation from rest leads to states with J = 0 to 2, but with a definite energy. For $\bar{p}p$ annihilation in flight, the angular momentum produced can range from J = 0 to $J \approx 5\sqrt{(MT_L/2)}$ for $\bar{p}$ with kinetic energy T_L incident on target p; thus up to $J \approx 11$ for $\bar{p}$ of momentum 10 GeV/c, for example. In pp interactions, the angular momentum can run as high as $J \approx 5\sqrt{s}/2$;

thus, up to $J \approx 150$ in ISR collisions. Clearly, e^+e^- annihilation allows the exploration of the characteristics of hadronic matter in a novel (and hopefully simpler) situation.

The models we have for these phenomena give few quantitative predictions, and these models are quite uncertain. A knowledge of the actual phenomena is needed in order that we may deduce what are in fact the major physical effects operating. The beam energy E = 14 GeV proposed for EPIC will be high enough to lead to very substantial progress on all these questions. Even if the total hadronic cross sections are only comparable with (2), that for the leptonic process $e^+e^- \rightarrow \mu^+\mu^-$, the hadron event rate at the EPIC energy would be 10 events/hour at the design luminosity $\mathcal{L} = \frac{1}{4} \times 10^{32}\ cm^2 sec^{-1}$, which would still allow this experimental programme to be carried out fully.

b) Quantum Electrodynamics (QED)

The validity of QED is of obvious importance in all experimentation with EPIC, and this must necessarily be tested carefully. Deviations from QED will certainly be found, due to

(i) hadronic (vacuum) polarization effects. These are largely calculable from (3) using the data on the ratio (1) deduced in EPIC experiments,

(ii) weak interaction effects, to be discussed below.

The most detailed test of QED will be provided by the study of the Bhabha scattering $e^+e^- \rightarrow e^+e^-$, a process which is spacelike-dominated, and which is consequently relatively insensitive to the (calculable) hadronic effects and to the weak interactions. The processes $e^+e^- \rightarrow e^+e^-\gamma$ and $e^+e^-\gamma\gamma$ will both merit detailed study, also. The process $e^+e^- \rightarrow \mu^+\mu^-$, being timelike-dominated, must also be checked from this viewpoint, although far more sensitive

to the two deviations just mentioned.

c) Weak Interaction Effects.

It is now well-established that the weak interactions include terms with neutral currents. It is generally believed that their occurrence is bound up with the unification of weak (Wk) and electrodynamic (EM) interactions proposed in outline many years ago by Salam-Ward and in full detail recently by Weinberg who made it part of a finite gauge theory of these interactions. In these theories, the EM and Wk interactions have comparable strengths at sufficiently high energies. The EPIC energy is well below these energies, but sufficiently high that substantial effects are to be expected to arise from interference between the effects of these two interactions. However, the weak interactions include terms which violate reflection (P) and charge-conjugation (C) invariance, and so characteristic P- and C-violation effects are expected to occur, arising from these interferences. At EPIC energies, the effects anticipated will have asymmetry coefficients typically of order 10%.

The most straightforward observations will be those indicative of C-violation, for example as a backward-forward asymmetry in the reaction $e^+e^- \rightarrow \mu^+\mu^-$. Such an asymmetry can arise from the C-invariant EM interactions alone, in consequence of interference between one-photon and two-photon interactions, and of the bremsstrahlung processes, but these EM effects are completely calculable and can be allowed for. P-violation effects would be quite unmistakable in their character, and can arise in no other way, but the most accessible effects require the use of e^+ and e^- beams with polarization, the most convenient situation being that in which one incident beam has longitudinal polarization, the other beam being either unpolarized or polarized parallel to the first beam. Even

those effects which do not involve P- or C-violation are identifiable, through their characteristic energy dependence - roughly speaking, the EM amplitude has energy-dependence $1/E^2$, whereas the Wk amplitude is essentially E-independent, in the EPIC energy range, so that the Wk effects will appear as a growing deviation from QED, with a characteristic E-dependence. The aim of these studies is to deduce detailed properties of the neutral current interactions, which it may prove difficult to deduce from the less complete studies to be made with high-energy neutrino beams interacting with proton, neutron and electron targets.

The process of primary interest for these studies is $e^+e^- \to \mu^+\mu^-$. Here the effects of interest are relatively strong because the EM process occurs only through the one-photon annihilation graph of Fig. 4(a). These effects are also of interest in the stronger process $e^+e^- \to e^+e^-$, which is mediated by both graphs (a) and (b) of Fig. 4, although the asymmetry coefficients are then at the 1% level, at EPIC energies. These phenomena will also be of much interest for other inclusive processes, such as $e^+e^- \to \bar{p}p$ (and especially $\bar{\Lambda}\Lambda$ and $\bar{\Sigma}^+\Sigma^+$), if their cross sections turn out to be large enough, or for the inclusive processes of the type $e^+e^- \to \pi X$, pX', $\Lambda X''$, etc., which can certainly be studied. All of these studies would benefit enormously from a longitudinal polarization capability for the electrons and positrons. Antiparallel transverse polarizations are produced automatically for the electron and positron beams, by the effect of synchrotron radiation, under suitable circumstances. The most convenient devices which can be designed to rotate these polarizations from transverse to to longitudinal configurations lead most naturally to antiparallel longitudinal polarizations for the colliding electron and positron beams. It is desirable to be able further to transform these to give parallel longitudinal polarizations, or to destroy the polarization of one

beam before collision, in order to introduce a spin asymmetry into the e^+e^- colliding system.

A search for heavy leptons up to mass 14 GeV at least will also be possible, Unified gauge theories allow the possibility of heavy fundamental leptons within this mass range, but they do not require them at present. Their production would be most direct through the pair production process

$$e^+e^- \rightarrow L^+L^-, \qquad (5)$$

followed by the decay processes $L^\pm \rightarrow \mu^\pm + \nu_\mu + \nu_L$. Their mass value would be determined from observation of muon production rates as a function of beam energy E, being indicated by a rapid rise in rate as the energy E rises through the threshold for the process (5). Any evidence found for such heavy leptons would represent a real breakthrough in our knowledge of leptons.

d) Non-annihilation production processes

These processes are characterized by the graph Fig. 1(b). The amplitude for the process

$$e^+ + e^- \rightarrow e^+ + e^- + X \qquad (6)$$

factorizes into two elements. The first is electrodynamic, the relation of the virtual photons with the electron and positron, which is entirely QED, and the second is hadronic, associated with the cross section for the "two-photon process"

$$"\gamma" + "\gamma" \rightarrow X, \qquad (7)$$

the final states X being limited to those with charge-conjugation parity C = +1. This cross section, averaged over all photon polarizations, may be written $\sigma_{\gamma\gamma X}(k_1^2, k_2^2, s)$, where k_1^2 and k_2^2 denote the effective masses for the virtual photons and s denotes $(\text{energy})^2$ for the hadron system X, specified in its rest frame.

The total cross sections calculated for these processes are large and increase with energy, as shown on Fig. 5. The major contributions to the cross sections arise from "almost real" photons and these are weighted strongly in favour of low s-values. Thus, a large part of the total cross section can be understood in terms of the "effective photon spectrum" $F(\omega)d\omega$, given by

$$F(\omega) = \frac{2\alpha}{\pi\omega}\left\{\left(1-\frac{\omega}{E}+\frac{\omega^2}{2E^2}\right)\ln\left(\frac{E}{m_e}\left(\frac{1-\omega/E}{1-\omega/2E}\right)\right)+\frac{\omega^2}{4E^2}\ln\left(\frac{2E}{\omega}-1\right)-\left(1-\frac{\omega}{E}\right)\right\}, \qquad (8)$$

the leading term being given by the coefficient of $\ln(E/m_e)$. The $\gamma\gamma \to X$ process is then due to the interaction of photons of energies ω_1 and ω_2 moving along the beam directions, the value of s being given by $s = 4\omega_1\omega_2$. The total cross section is then approximated by

$$\sigma = \int d\omega_1 d\omega_2 F(\omega_1)F(\omega_2)\sigma_{\gamma\gamma X}(k_1^2=k_2^2=0, s=4\omega_1\omega_2) \qquad (9)$$

For orientation, consider the case $\sigma_{\gamma\gamma X}$ = constant; the integral over ω_1 and ω_2 gives

$$\int d\omega_1 d\omega_2 F(\omega_1)F(\omega_2) = 0.064 \qquad (10)$$

at the EPIC energy E = 14 GeV. Next, approximate $F(\omega)$ by the leading term $(2\alpha/\pi\omega)\ln(E/m_e)$ in (8). Then the integral can be carried out for fixed s, to give

$$\frac{d\sigma}{ds} = \left(\frac{2\alpha}{\pi}\ln\left(\frac{E}{m_e}\right)\right)^2 \frac{\ln(4E^2/s)}{s}\,\sigma_{\gamma\gamma X}(s). \qquad (11)$$

This weighting of the cross section towards low s is well illustrated by an exact calculation for $e^+e^- \to (e^+e^-+\text{hadrons})$, whose s distribution is shown on Fig. 6. This dominance of low s is extreme for the case $e^+e^- \to e^+e^-e^+e^-$, but the created electrons have dominantly such low s values that they are too slow to cause background trouble or else are swept out along the beam directions. Although low s is dominant for μ pair production and for hadron

production, the produced particles are not dominantly swept out along the beam directions, but they do have rather low energies in the e^+e^- laboratory frame. For the muons from the process $e^+e^- \rightarrow e^+e^-\mu^+\mu^-$, treated in the "effective photon approximation", the shape of the p_L distribution is depicted on Fig. 7, for various p_T values; the spread in p_L is at most comparable with p_T, being much less than this for high p_T. The p_T distribution, integrated over all p_L, is shown on Fig. 8; this peaks for a rather low value, $p_T \approx 0.07$ GeV/c. Since we see a clear physical origin for these conclusions, we can accept them as typical also for pions and can conclude that these "two-photon" processes (6) will give rise to little confusion with the "one-photon" processes (1).

These "two-photon" processes (6) allow access to interesting physics information difficult to achieve in other ways, concerning the electromagnetic interactions of low-mass C = +1 resonances. A few specific processes of interest may be listed as follows,

$$\text{"}\gamma\text{"} + \text{"}\gamma\text{"} \rightarrow \pi^0 \text{ (or } \eta\text{, or } \eta'\text{)}, \tag{12a}$$

$$\rightarrow \epsilon \text{ (or f)} \rightarrow \pi^+\pi^-, \tag{12b}$$

$$\rightarrow A2 \rightarrow \rho\pi, \tag{12c}$$

$$\rightarrow S^* \rightarrow K^+K^-. \tag{12d}$$

Clearly, for broad meson resonances M, the coupling $M \rightarrow \gamma\gamma$ is difficult to measure by other means.

Because of the dominance of low s events, a large part of the physical information contained in the processes (6) at EPIC energies will already have been explored in data at lower electron energies (at Frascati and at SPEAR). The new information at EPIC will be concerned with

i) $\sigma_{\gamma\gamma X}(s)$ for large s, above the narrow resonance region,

ii) $\sigma_{\gamma\gamma X}(k_1^2, k_2^2, s)$ for low s but for large values of k_1^2 (or k_2^2 or both). This includes the interesting regime of deep-inelastic scattering of an electron off a virtual photon.

To obtain the latter information, it will be necessary to tag either or both the scattered electron and positron. Two difficulties are conceivable about tagging here:

(a) the high cross sections for purely electrodynamic processes, which give rise to copious electrons and positrons at small angles (typically of order m_e/E_e) to the beam direction,

(b) the small duty cycle for interaction between the beams. The collision time between an electron bunch and a positron bunch is of order 10^{-9} sec., which makes it impossible to separate unrelated events occurring within the same burst, by use of timing. There are about 3×10^6 bursts per second, so that different bursts are well separated in time.

It would be difficult to tag all events, because of accidental coincidences due to the first difficulty (a). However, it should be possible to tag events in which the electron (and/or positron) angles exceed about $\theta_o = 0.015$ radians, which corresponds to k^2 values exceeding about $0.04\ (\mathrm{GeV}/c)^2$. Such tagging has been used successfully at SLAC, where the effective luminosity is much greater ($\times 10^2$) than that for EPIC. We may note here also that double tagging of "$\gamma\gamma$" events has been achieved with small angle tagging and with energy measurement of the electron and positron energies at Frascati ($E_e = 1.5$ GeV), at a luminosity of $10^{30}\mathrm{cm}^{-2}\mathrm{sec}^{-1}$.

The second difficulty (b) is not serious for EPIC. To give some feel for the situation, it will be useful to give some event rates, appropriate to the EPIC energy and luminosity $\mathcal{L} = \frac{1}{4} \times 10^{32}\mathrm{cm}^{-2}\mathrm{sec}^{-1}$:

i) Bhabha scatterings through angles $\theta \geqslant \theta_0$ occur at a rate about 10^{-3}/burst.

ii) e^+e^- bremsstrahlung with emission of a photon exceeding 1 GeV and of an electron or positron with angle $\theta \geqslant \theta_0$ has a rate about 10^{-4}/burst.

iii) the "$\gamma\gamma$" process "$e^+e^- \rightarrow e^+e^-$ hadrons" occurs with a total rate about 2×10^{-6}/burst. If one electron or positron is tagged with $\theta \geqslant \theta_0$, this rate falls to 6×10^{-7}/burst; when both electron and positron are tagged, the rate is about 4×10^{-8}/burst.

iv) the annihilation process "$e^+e^- \rightarrow$ hadrons" would have a rate of 2×10^{-6}/burst if the total cross section $\sigma(e^+e^- \rightarrow$ hadrons) were to remain at 20 nb. If this cross section were equal to $\sigma(e^+e^- \rightarrow \mu^+\mu^-)$, the annihilation process would occur at rate 9×10^{-9}/burst.

Our conclusion is that double tagging does appear feasible at EPIC, in principle, at least for large angles $\theta \geqslant \theta_0 \approx 0.015$ rad. However, experience with SPEAR suggests that the backgrounds dangerous to tagging may come from beam-gas and beam-wall collisions, which we cannot anticipate at present for EPIC. With double tagging, it will be possible to measure the three variables k_1^2, k_2^2 and s for each event. Since the plane of the electron (positron) scattering defines the polarization of each virtual photon, double tagging will also allow the separation of the cross sections $\sigma^{\parallel}_{\gamma\gamma X}$ and $\sigma^{\perp}_{\gamma\gamma X}$. The use of polarized electron and positron beams will allow still further detail of the processes (6) to be probed.

The members of EPIC Working Party 1 were as follows:

D. Bailin	E. Gabathuler
R. Budny	D. Lyth
G. Conforto	A. McDonald
N. Cottingham	D. Morgan
R. H. Dalitz (Chairman)	A. Segar
N. Dombey	W. Toner

Figure Captions

1. The Feynman graphs (a) and (b) depict the processes of (a) particle production in e^+e^- one-photon annihilation, and (b) particle production in e^+e^- inelastic scattering possible with two-photon exchange.

2. The data available for the ratio $R(4E^2) = \sigma(e^+e^- \to \text{hadrons})/\sigma(e^+e^- \to \mu^+\mu^-)$ are plotted as function of the beam energy E. It is a long and uncertain extrapolation from the highest energy point here to the EPIC energy E = 14 GeV.

3. The total cross sections $\sigma(e^+e^- \to \text{hadrons})$ measured to date are plotted as function of the beam energy E. It is a long and uncertain extrapolation from these data to the EPIC energy E = 14 GeV.

4. The Feynman graph (a) depicts the one-photon annihilation graph appropriate for Bhabha scattering (e^+e^- elastic scattering) and for the reaction process $e^+e^- \to \mu^+\mu^-$. In this graph the photon is time-like. The Feynman graph (b) depicts the process of

photon exchange which contributes to the Bhabha scattering amplitude, but which has no counterpart for the process $e^+e^- \to \mu^+\mu^-$. Here the photon transferred is space-like.

5. The total cross sections for various two-photon processes are plotted as function of the electron beam energy E, together with the cross section for the one-photon annihilation process $e^+e^- \to \mu^+\mu^-$. The dashed curve represents an exact calculation (i.e. not limited to the "effective photon approximation", but taking into account fully the correct kinematics, both for the matrix-element and for phase space) for the final state $e^+e^-\pi^+\pi^-$. This curve is to be compared with the solid curve shown for the same final state, which was calculated in the effective photon approximation. The cross section for hadronic states with mass $\geqslant 1$ GeV was calculated assuming that the total cross section $\sigma(\gamma\gamma \to \text{hadrons})$ has the constant value 0.25 μb obtained by appeal to Regge factorizability and the empirical values for the total cross sections $\sigma(\gamma p \to \text{hadrons})$ and $\sigma(pp)$ in the high energy region.

6. The distribution of s for the final hadrons (s = (invariant mass)^2 for all the hadrons) is plotted for two classes of final state, as calculated in the effective photon approximation, for the case of beam energy E = 10 GeV. The cross section including all hadronic states with mass $\sqrt{s} \geqslant 1$ GeV was calculated assuming that the total cross section $\sigma(\gamma\gamma \to \text{hadrons})$ had the constant value 0.25 μb obtained by appeal to Regge factorizability and the empirical pp and γp total cross sections.

7. For the process $e^+e^- \to e^+e^-\mu^+\mu^-$, the form of the longitudinal momentum (p_L) distribution (normalized to unity for $p_L=0$) for an outgoing muon is shown as function of the transverse momentum p_T carried by this muon, as calculated in the effective

photon approximation for beam energy E = 14 GeV.

8. For the process $e^+e^- \rightarrow e^+e^-\mu^+\mu^-$, the distribution of the transverse momentum p_T for an outgoing muon (integrated over the p_L distribution for this muon) is shown, as calculated in the effective photon approximation, for beam energy E = 14 GeV.

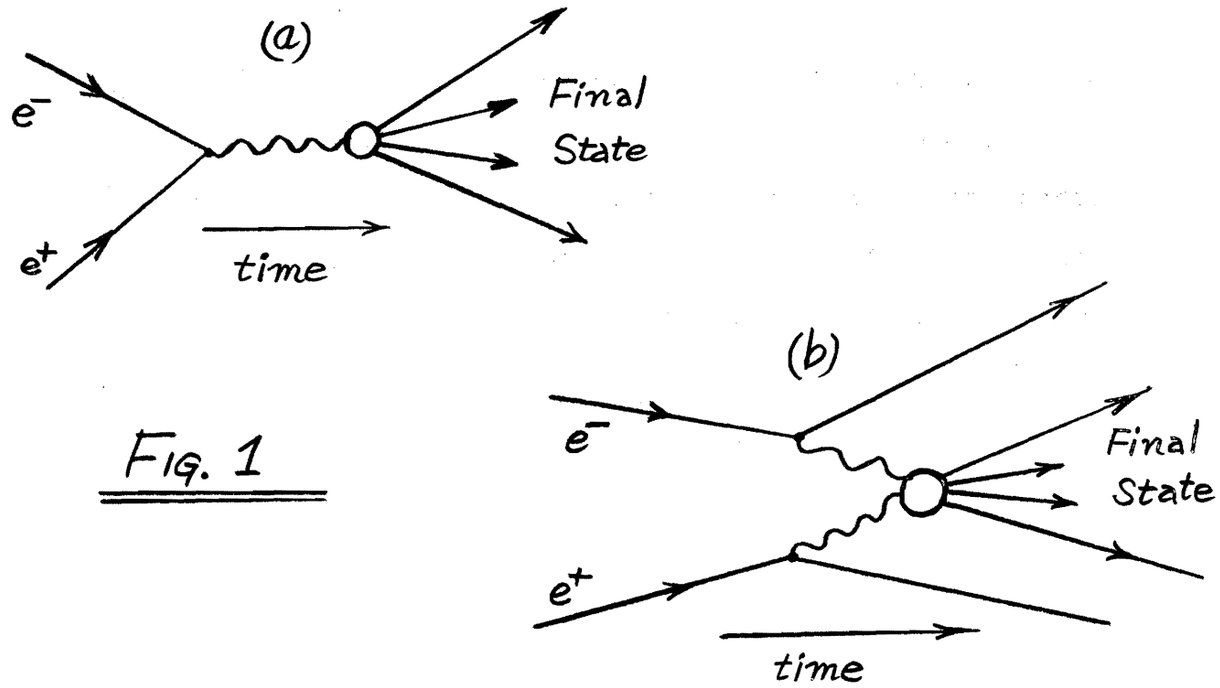
(a)
e⁻
e⁺
Final
State
time
(b)
e⁻
e⁺
Final
State
time

FIG. 1

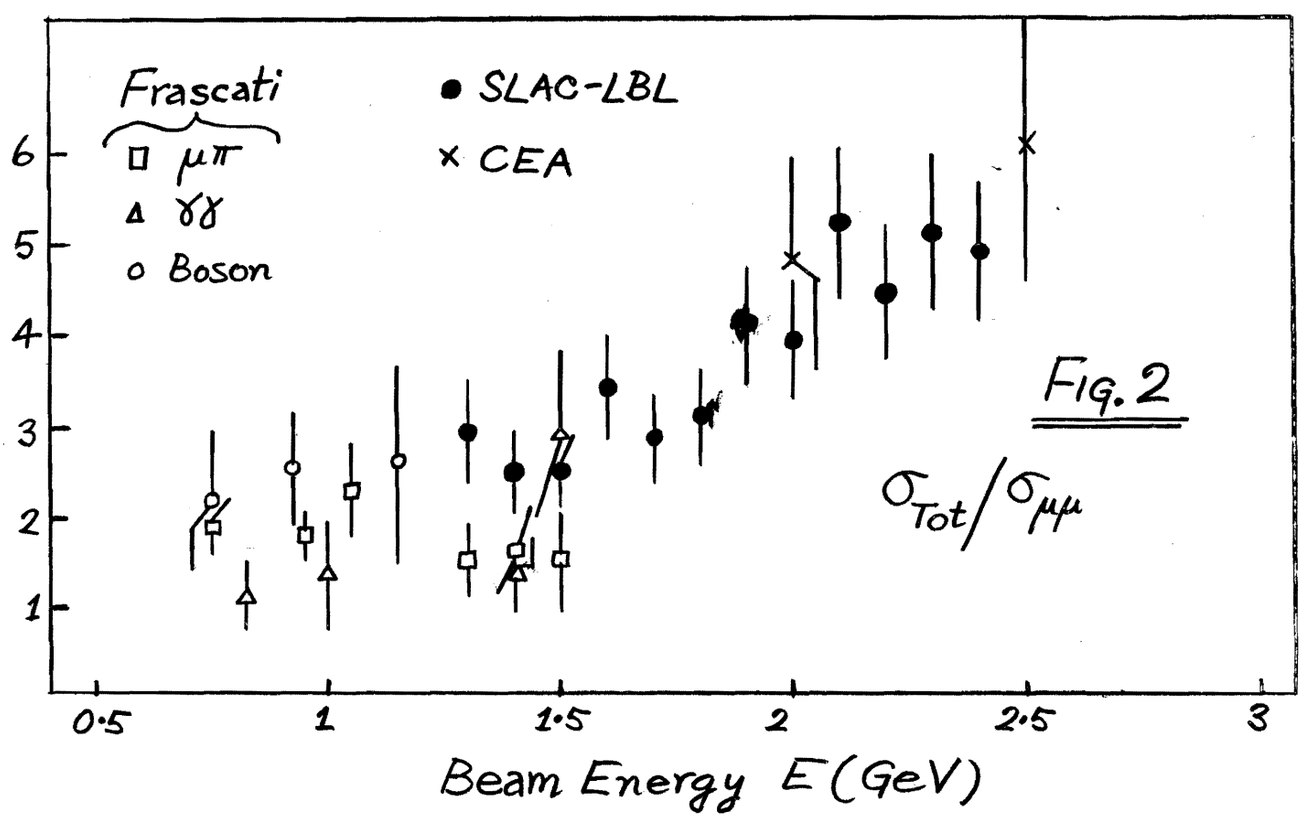
Frascati
□ μπ
△ γγ
○ Boson
● SLAC-LBL
× CEA
6
5
4
3
2
1
0·5
1
1·5
2
2·5
3
Beam Energy E (GeV)
σTot/σμμ

FIG. 2

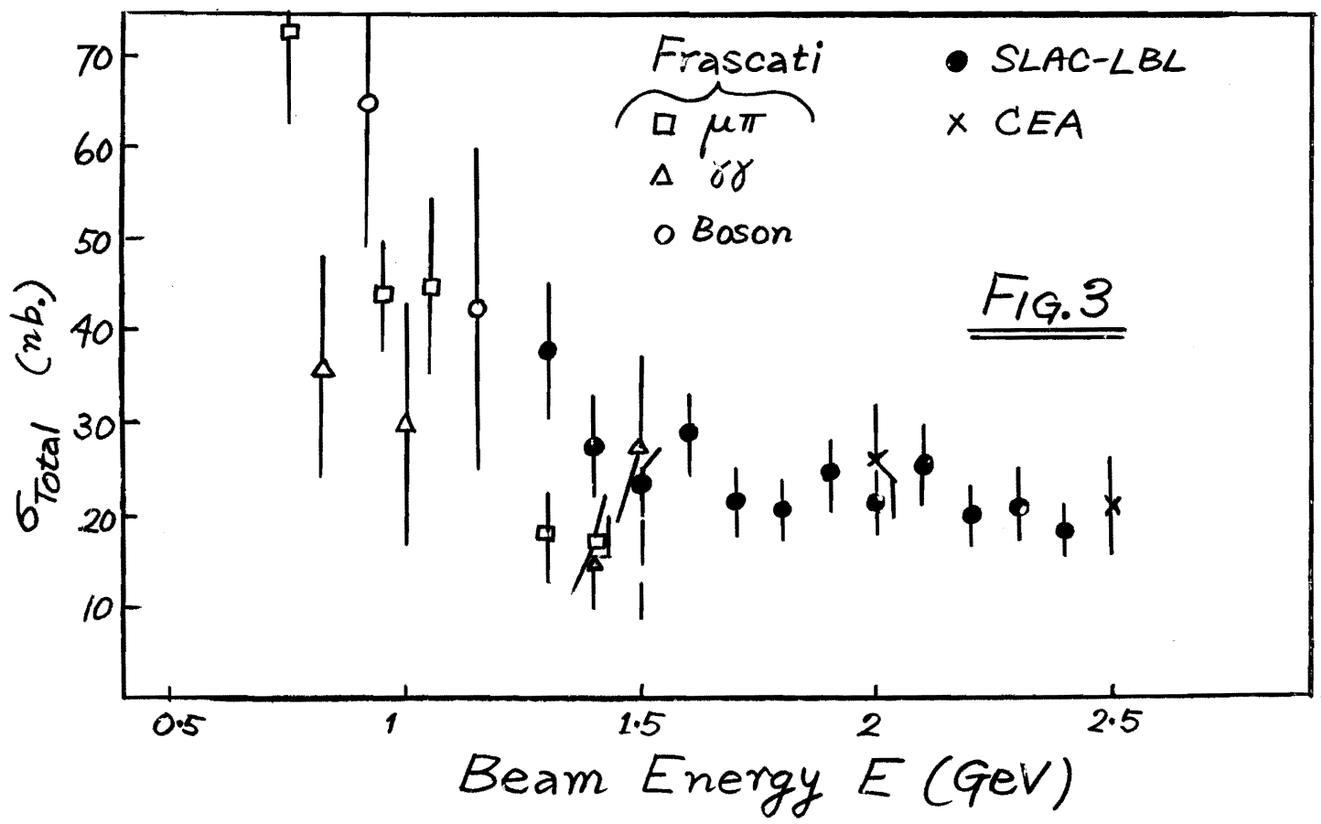
Frascati
□ μπ
△ γγ
○ Boson
● SLAC-LBL
× CEA
70
60
50
40
30
20
10
σTotal (nb.)
0·5
1
1·5
2
2·5
Beam Energy E (GeV)

FIG. 3

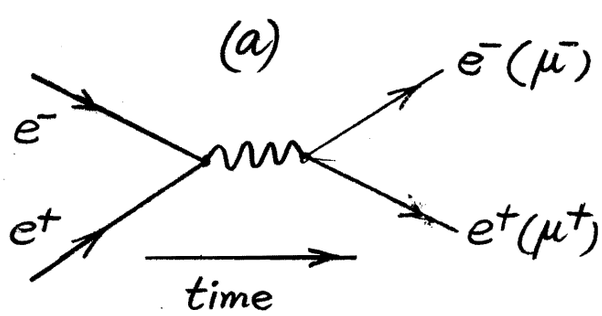
(a)
e⁻
e⁺
e⁻(μ⁻)
e⁺(μ⁺)
time

FIG. 4

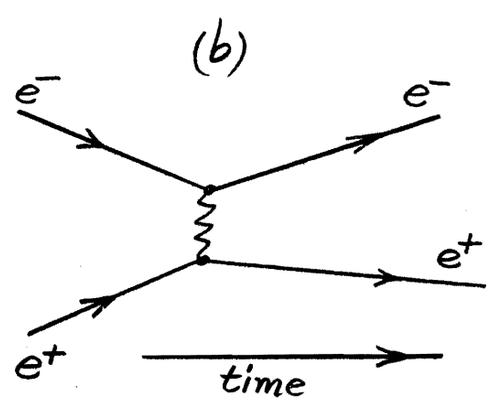
(b)
e⁻
e⁻
e⁺
e⁺
time

Fig. 5

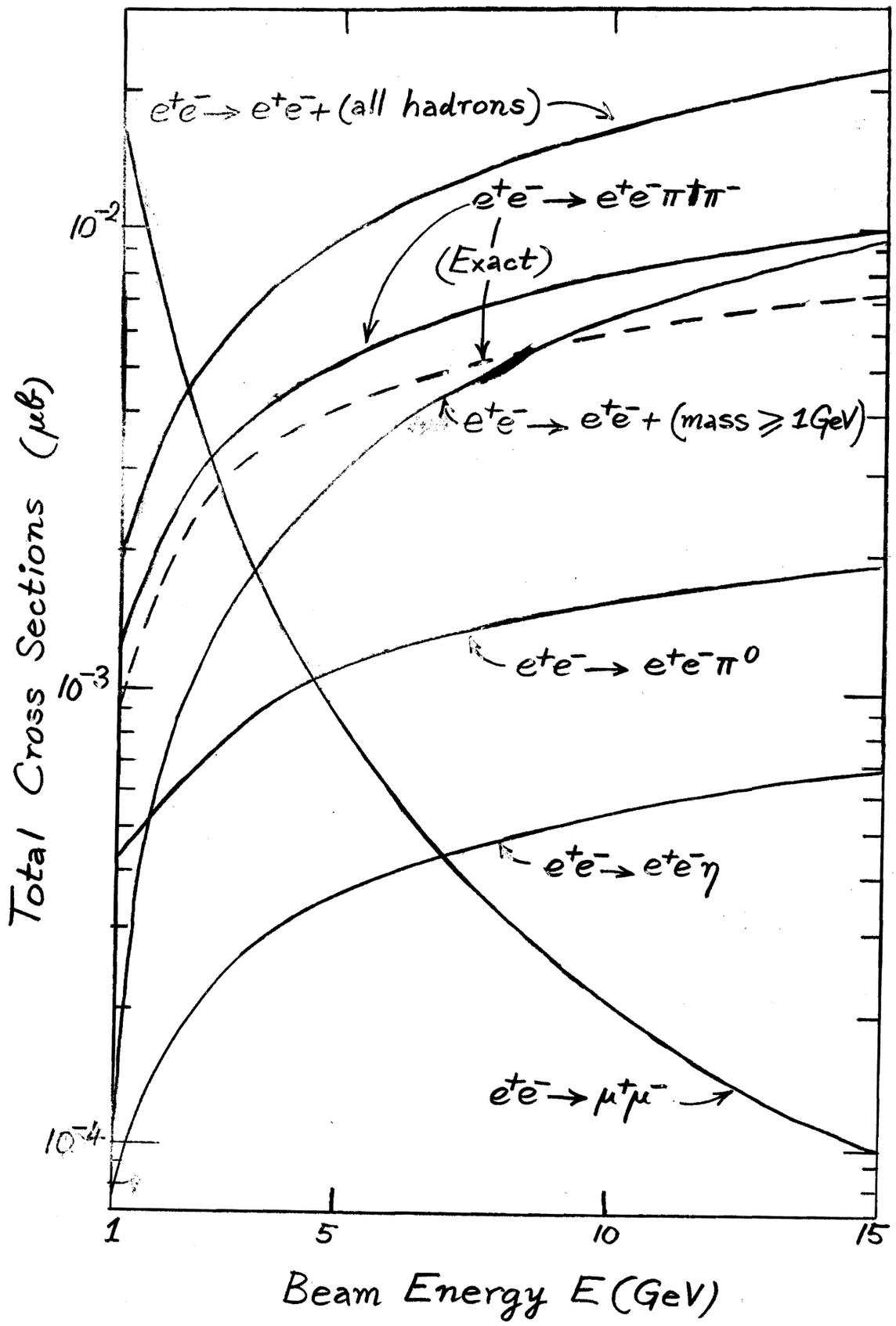
$e^+e^- \to e^+e^-$ + (all hadrons)
$e^+e^- \to e^+e^-\pi^+\pi^-$
(Exact)
$e^+e^- \to e^+e^-$ + (mass $\geq$ 1GeV)
$e^+e^- \to e^+e^-\pi^0$
$e^+e^- \to e^+e^-\eta$
$e^+e^- \to \mu^+\mu^-$
10^{-2}
10^{-3}
10^{-4}
Total Cross Sections (μb)
1
5
10
15
Beam Energy E (GeV)

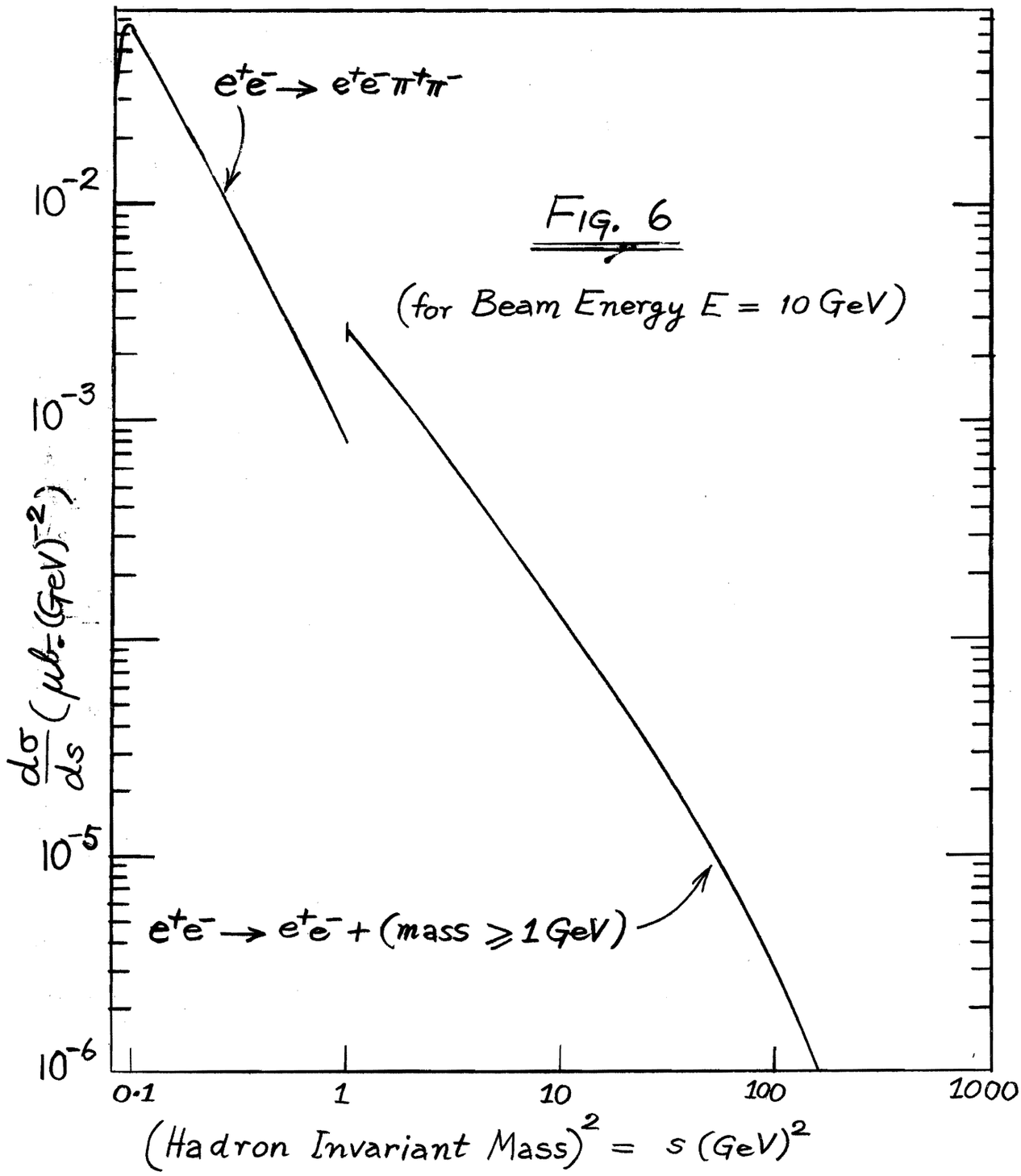

FIG. 6

(for Beam Energy $E = 10$ GeV)

FIG. 7 The process $e^+e^- \rightarrow e^+e^-\mu^+\mu^-$ for $E = 14$ GeV.

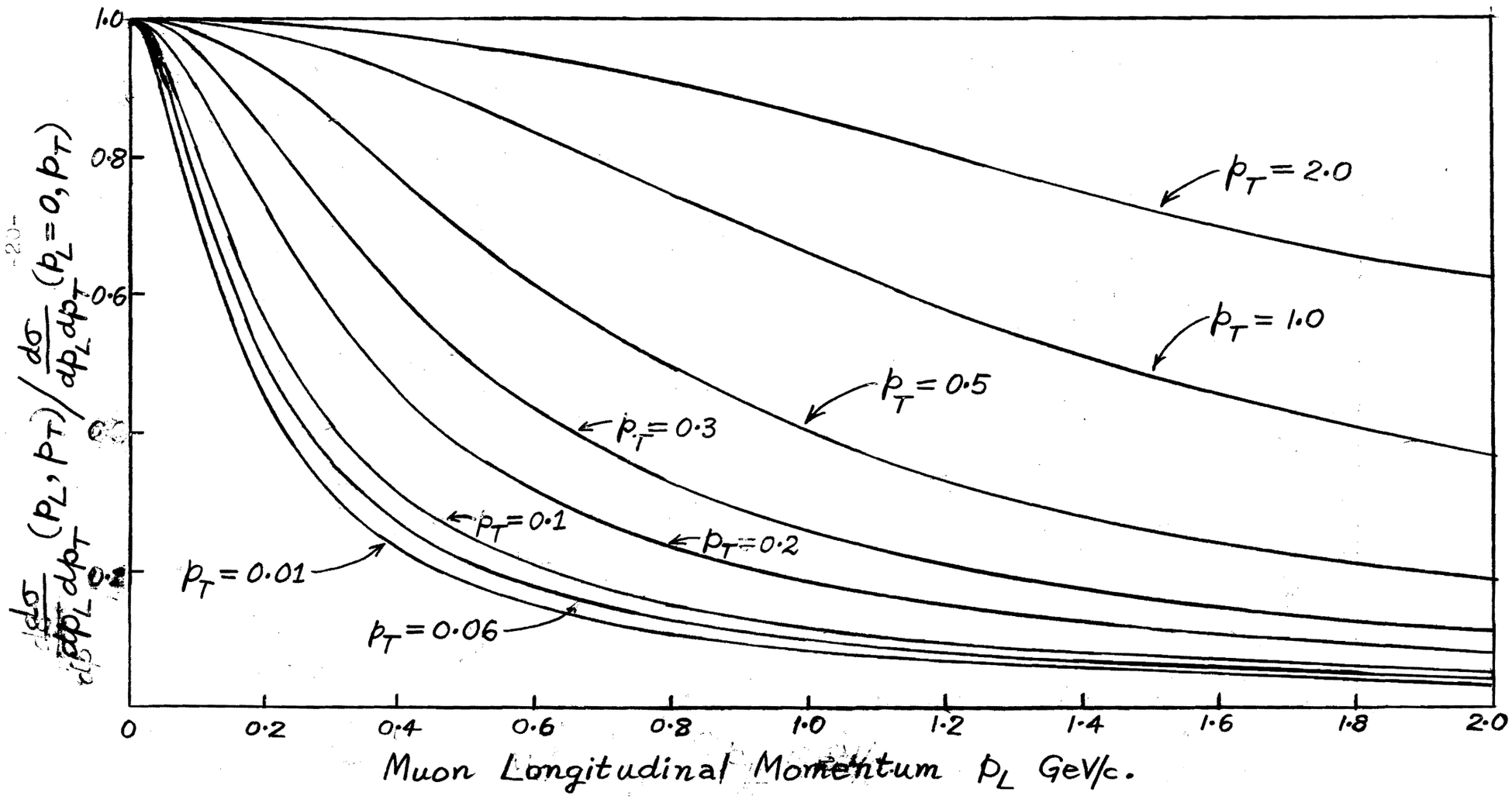

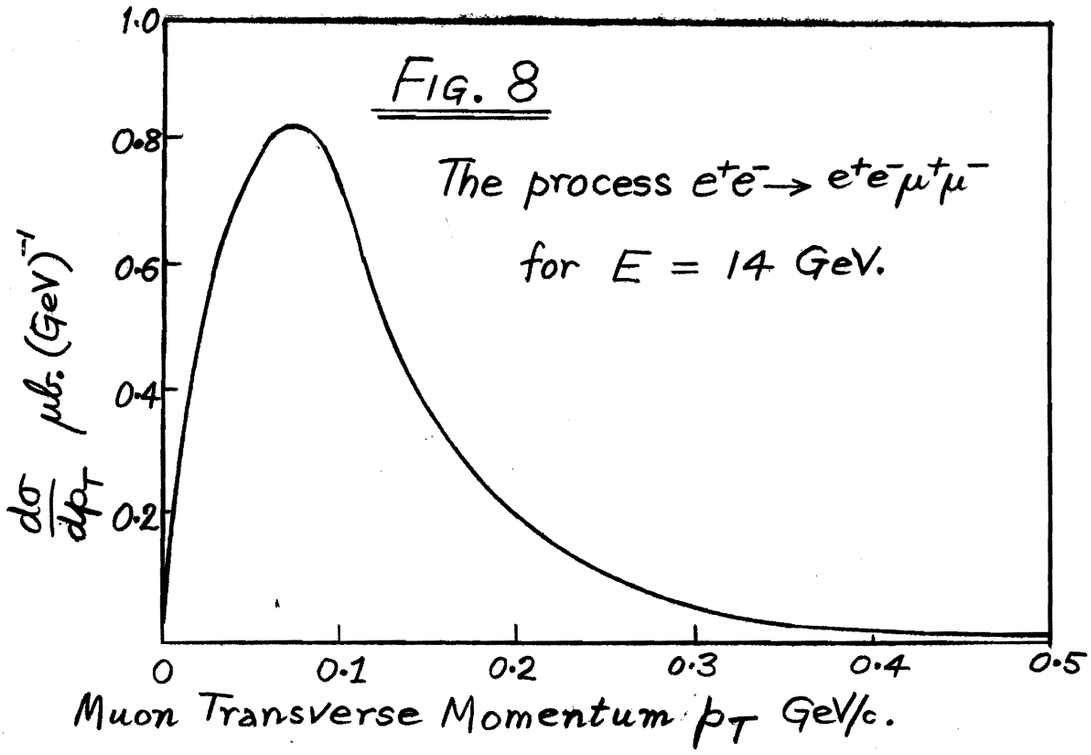
FIG. 8
The process $e^+e^- \rightarrow e^+e^-\mu^+\mu^-$
for $E = 14$ GeV.
1.0
0.8
0.6
0.4
0.2
$\frac{d\sigma}{dp_T}$ μb. (GeV)$^{-1}$
0
0.1
0.2
0.3
0.4
0.5
Muon Transverse Momentum p_T GeV/c.